Electronic Research Archive

ERA, 30(12): 4256–4276.
DOI: 10.3934/era.2022217
Received: 29 August 2022
Revised: 18 September 2022
Accepted: 19 September 2022
Published: 27 September 2022

http://www.aimspress.com/journal/ERA

Research article

Analysis of bus travel characteristics and predictions of elderly passenger flow based on smart card data

Gang Cheng[1,3,*] and Changliang He[2,3]

[1] College of Engineering, Tibet University, Lhasa 850000, China
[2] College of Information Science and Technology, Tibet University, Lhasa 850000, China
[3] Center of Tibetan Studies (Everest Research Institute), Tibet University, Lhasa 850000, China

* **Correspondence:** Email: fengyunleng@163.com.

Abstract: Preferential public transport policies provide an important social welfare support for travel by the elderly. However, the travel problems faced by the elderly, such as traffic congestion during peak hours, have not attracted enough attention from transportation-related departments. This study proposes a passenger flow prediction model for the elderly taking public transport and validates it using bus smart card data. The study incorporates short time series clustering (STSC) to integrate the elements of the heterogeneity of bus trips taken by the elderly, and accurately identifies the needs of elderly passengers by analysing passenger flow spatiotemporal characteristics. According to the needs and characteristics of passenger flow, a short time series clustering Seasonal Autoregressive Integrated Moving Average (STSC-SARIMA) model was constructed to predict passenger flow. The analysis of spatiotemporal travel characteristics identified three peak periods for the elderly to travel every day. The number of people traveling in the morning peak was significantly larger compared to other periods. At the same time, compared with bus lines running through central urban areas, multi-community, and densely populated areas, the passenger flow of bus lines in other areas dropped significantly. The study model was applied to Lhasa, China. The prediction results verify that the model has high prediction accuracy and applicability. In addition to the initial application, this predictive model provides new directions for bus passenger flow forecasting to support better public transport policy-making and improve elderly mobility.

Keywords: elderly travel; bus passenger flow; STSC-SARIMA model; spatiotemporal characteristics; passenger demand; passenger flow forecast

1. Introduction

As people live longer, populations around the world are aging faster, impacting almost every aspect of society. Population aging is a continuing trend in societal development, especially in developing countries. Most developing countries are facing the pressures of aging including China, which has already become an aging society. In response to these problems, concessionary public transport schemes have been implemented around the world to improve the welfare of older people. For example, in London, in the United Kingdom (UK), older people aged 60 and over are entitled to free bus travel. In Beijing, China, local residents aged 65 and over take city buses for free throughout the year, which helps address peak travel pressure for the elderly [1]. Many studies have shown that preferential public transport policies can create public benefits for the elderly by improving their travel quality and increasing their mobility [2]. These benefits can also lessen the sense of social exclusion for recipients [3].

However, when policymakers formulate preferential policies for public transportation for the elderly, they often do not pay enough attention to temporal and spatial relationships, such as passenger flow and routes and the pressures faced during peak travel periods. For this reason, this research focuses on methods that can be adapted to alleviate the stress of traveling for older people. There are significant differences in the spatial and temporal travel characteristics of different groups, with older people traveling less frequently, over shorter distances, and starting their journeys later compared to younger people [4]. The population distribution of young and old is geographically similar, and the lifestyles of the elderly tend to be fixed. Due to their poor physical condition, the travel time of the elderly is mostly concentrated in the morning and to activities in specific board districts. The mobility of the elderly has increased significantly since the 21st century [5]. Experiments have shown that mobility is closely related to the quality of life of older people and that travel opportunities are important in influencing their travel satisfaction, and inner satisfaction is directly related to the physical health of the elderly [6−9].

Like most developing countries, China is currently at an intermediate level of economic development. As people age, they are abandoning private cars and inexpensive public transport is becoming increasingly popular among the elderly [10]. Some scholars have analysed the demand for public transport for older people during peak travel times as a way of proposing policies that would benefit their mobility [11]. However, most of these studies have focused on peak seasonal long-term travel patterns, and few articles have examined the characteristics of older people's public transport trips during short peak periods. It is, nonetheless, essential to analyse the characteristics of short-time trips and to locate the demand [12−14]. Given this background, this study focuses on the travel characteristics of elderly people aged 60 and above. A clustering method was used to classify peak hours, and the passenger load ratio was used as a metric to locate passenger demand. The seasonality of travel was also tested and eliminated, and ultimately a forecasting model was built using Seasonal Autoregressive Integrated Moving Average (SARIMA). The short time series clustering analysis in the study effectively extracts similarities within time periods and resolves irregular components in time series as a way of capturing the heterogeneity of the elderly population's activity during travel periods. Travel behavior is different for each elderly person, but the travel pattern is similar for the overall category of the elderly, who generally have homogeneous characteristics in society overall. The travel characteristics of older people with similar characteristics are often studied in categories that more accurately model their travel characteristics [15]. This research can benefit policymakers

and planners in developing measures based on specific target groups and provide effective recommendations for transport planning and policies to address public transport congestion for older adults, improving their mobility.

The paper is structured as follows. Section 2 presents a review of the relevant literature. Section 3 presents the research methodology and associated models. Section 4 describes the data sources. Section 5 presents the analysis results and validates the model with smart card data. Section 6 summarizes the study findings and proposes policies to improve bus travel among older adults.

2. Literature review

Passenger flow forecasting methods are mostly data-driven, using tools such as time series data. Forecasts can be divided into long-term forecasts and short-term forecasts based on the length of time. Long-term forecasts are mainly combined with data on land resources, demographics, and traffic surveys to forecast features of urban areas over long periods of time and are generally used for transport planning and construction [16]. By contrast, short-term passenger flow forecasting is more focused on people's daily trips and traffic operations; is usually expressed in terms of minutes, hours, and days; and is based on historical passenger flow data, often recorded by smart card systems [17,18].

Short-term passenger flow forecasting research has focused on rail, air, road, and water transport, mainly by extracting the temporal relationships between different variables from historical data to reasonably forecast future demand [19]. The main methods for creating short-term passenger flow forecasts include linear forecasting, non-linear forecasting, and combined forecasting. Linear forecasting methods reflect the intrinsic characteristics of the data in the form of parameters and capture the heterogeneity of the information contained in the time series by changing the parameters. These methods include Kalman filter models, exponential smoothing models, and autoregressive moving average (ARIMA) models [20,21]. The methods have the advantages of fully revealing the trends and cyclical characteristics of passenger flow, but the disadvantages of being more sensitive to the steady state of the data. As such, the complexity of the conditions may lead to decreased accuracy [22−24]. Non-linear prediction methods are mainly based on machine learning and include support vector machines [25], neural networks [26,27], XGBoost [28], and fuzzy neural networks [29]. The combined prediction method is a hybrid model that combines the first two types, using a linear model for initial prediction and then a non-linear model for correction. This type of model has the advantage of having a high accuracy of fit, but the disadvantages of being highly complex and having a long computation time [30,31].

As computer hardware conditions have matured, changes in the complexity of neural network structures have accelerated, leading to the formation and rapid development of deep neural networks. Fu et al. proposed a neural network model for short-term metro passenger flow prediction, which incorporates spatio-temporal features and contains data inputs from multiple sources [32]. Tang et al. proposed a multi-community spatio-temporal convolutional neural network framework for short-term passenger predictions for different communities in the same area to capture spatio-temporal correlation [16].

Short-term passenger forecasting for conventional public transport, which is part of road transport, is mostly studied using combined algorithmic models. Bai et al. proposed a multi-modal fusivity prediction algorithm, which gives significantly better results than a single algorithmic model [19]. Liu et al. proposed a hybrid deep neural network model, in which temporal features such as days of the week, hours of the day, and holidays, as well as average passenger flow, are used as inputs to define

elements of passenger flow, followed by short-term prediction of passenger flow. This approach generates a more accurate prediction of different passenger flow scenarios [33]. Luo et al. used a hash convolutional network to address the dynamic spatio-temporal correlation of bus routes, with the results showing that bus stops, routes, and spatio-temporal correlation are important factors affecting the accuracy of the prediction results [34]. In the area of short-term bus passenger forecasting, the performance of the combined forecasting models with neural networks is high; however, the accuracy cannot be improved due to an insufficient number of valid samples.

Bus smart card swipe data are widely used in travel studies to mitigate the shortage of valid samples and the difficulty of data collection. These data have been used for travel behaviour analysis and passenger demand forecasting [35−39]. In short-term passenger forecasting, combined linear forecasting methods do not require a large amount of training data, and the simplicity of the model and low computational complexity make it a promising approach for solving small sample forecasting problems. However, few practical studies have focused on models that consider a combination of spatio-temporal characteristics and combinatorial linear forecasting. Table 1 provides a descriptive summary of the most relevant and recent research on passenger flow forecasting using transit smart swipe card data.

Table 1. Research on short-term passenger flow forecasting models.

Author	Title	Main characteristics & results
Okutani and Stephanedes [40]	Dynamic prediction of traffic volume through Kalman filtering theory	Forecasting method based on Kalman filter theory, with complex models and suitable for real-time dynamic short-time forecasting
Min and Wynter [41]	Real-time road traffic prediction with spatio-temporal correlations	Smart transportation technologies have improved short-term passenger forecasting performance, but require large amounts of uninterrupted historical data
Chan et al. [42]	Neural-network-based models for short-term traffic flow forecasting using a hybrid exponential smoothing and Levenberg–Marquardt algorithm	Adding a neural network to a regression model for prediction improves generalization but increases model complexity
Xue et al. [43]	Short-term bus passenger demand prediction based on time series model and interactive multiple model approach	The interactive multi-model filtering algorithm model is a hybrid model; the prediction results are affected by a single model, and an optimal model needs to be found
Toqué et al. [44]	Short & long term forecasting of multimodal transport passenger flows with machine learning methods	Machine learning models have advantages in solving the problem of passenger flow forecasting in multimodal transport
Li et al. [45]	Forecasting bus passenger flows by using a clustering-based support vector regression approach	Nonlinear models combined with clustering can improve prediction accuracy
Jiao et al. [46]	Multi-step Time Series Forecasting of Bus Passenger Flow with Deep Learning Methods	The LSTM-GRU multi-step prediction model with reduced parameters can appropriately reduce the computational complexity
Lv et al. [47]	A Bus Passenger Flow Prediction Model Fused with Point-of-Interest Data Based on Extreme Gradient Boosting	The XGBoost algorithm model, which has the advantage of being robust, efficient, and scalable

There remain opportunities to improve the prediction accuracy of existing passenger flow prediction models using bus smart card data, and to improve their transferability. Some scholars have used a single model for passenger flow forecasting, focusing on the fitting effect and not considering the spatial and temporal correlation characteristics of passenger flow. Based on significant historical data about elderly people's public transport trips, this paper analyses elderly people's trips in the time dimension, the spatial dimension based on bus routes, and seasonal influencing factors. The study applies a short time series to dynamically adjust parameters to capture the irregular part of the time series, and establishes a uniform sample and database for model use and validation, improving the applicability of the model. This method offers a new approach to identifying steps that may improve travel for older people, relieve traffic congestion during peak travel times, and support public transport operations.

3. Methodology

As traffic information technology has developed, smart card data have become increasingly used for traffic payments, and many scholars have used these data to replace traditional types of data to study public travel by the elderly [48,49]. Several researchers have used the temporal information contained in smart card data to analyse the temporal changes in residents' public transport travel behaviour and the associated long-term effects of changes in environmental factors [50]. This paper proposes a method for forecasting the demand for short-term elderly public transport trips, using a seasonal differential autoregressive moving average model with short time series clustering. The method first uses basic travel characteristics to identify sources of demand and then removes seasonal effects through a moving average formula. Second, passenger load factors are combined with the spatial distribution of elements, such as population concentration, to comprehensively validate passenger demand. Finally, a SARIMA forecasting model is developed in conjunction with travel characteristics. The specific steps are as follows.

Step 1: Database construction

Step 1.1: Data cleansing. Data cleansing is mainly done to detect outliers. The Grubbs test is applied to detect outliers, with detected outliers treated as missing values [51]. In this paper, missing values are treated using the missing value substitution method as applied to time series. Missing values are filled in using a combination of the arithmetic mean and median, and the linear interpolation of the neighbourhood of missing values.

Step 1.2: Process the data in steps of months, days, and minutes. The distance short time series (STS) clustering algorithm is incorporated when processing minute-level data [52]. The time series is treated as a segmented linear function and the slope is measured. The number of older people taking public transport in each time period is denoted $x = [x_0, x_1, \cdots, x_{nt}]$, where x_{nt} is the cumulative number of people in that time period. Two consecutive time points $t_{(k)}$ and $t_{(k+1)}$ are artificially set; between them is a linear function $x(t)$ denoted $x(t) = \alpha_k t + b_k$, where $t_{(k)} \le t \le t_{(k+1)}$. The parameters α_k and b_k are calculated using Eqs (1) and (2):

$$\alpha_k = \frac{x_{(k+1)} - x_k}{t_{(k+1)} - t_{(k)}} \tag{1}$$

$$b_k = \frac{t_{(k+1)}x_k - t_k x_{(k+1)}}{t_{(k+1)} - t_k} \tag{2}$$

The STS distance is defined by calculating the square root of the sum of squares of the slope differences obtained from the linear function. The STS distance between the two time series x_1 and x_2 is defined using Eq (3):

$$d^2(x_1, x_2) = \left(\frac{x_{2(k+1)} - x_{2k}}{t_{(k+1)} - t_k} - \frac{x_{1(k+1)} - x_{1k}}{t_{(k+1)} - t_k}\right)^2 \tag{3}$$

Next, n days of data in the study months are randomly selected and the TST distance is calculated, where the value of n depends on the periodic value (T) of the periodic changes in the data over several days, and the calculated TST distance is averaged. At the same time, the number of passengers must be limited, namely $P \leq m$. The calculations are expressed in Eqs (4) and (5):

$$\bar{d}_i = \frac{\sum_1^n d_{TST}}{n}, n = C(n, 2) \tag{4}$$

$$\alpha = \frac{\bar{d}_i}{N_M}, P \leq m \tag{5}$$

In the formula, $\bar{d}_i$ denotes the average of the TST distances for the same time period on any two different days of a randomly selected n days in each month, α denotes the parameter of the clustering module, N_M is the total number of months selected, P denotes the number of people who swiped cards during that time period, and m denotes the number of people who set the maximum.

Step 1.3: Line identification. The method first identifies the route labels contained in each piece of data, and then classifies bus routes by traversing all the data. A unified database is constructed in conjunction with clustering methods to profile the travel, predict passenger flow, and validate model accuracy.

Step 2: Travel feature mining

Step 2.1: The database is used to analyse travel time characteristics and seasonal factors; and trend elements and cyclical fluctuations in travel are extracted. This study selected HP (Hodrick and Prescott) filtering and BP (frequency filter) filtering methods to decompose trend and cyclic elements [53].

Step 2.2: Calculate the load factor of bus routes regarding elderly passenger flows, rank using principal component analysis, and validate the travel demand by combining spatial factors, such as population clusters. The load factor is calculated using Eq (6):

$$P_{j,i} / \sum_{j=1}^{n} P_{j,i} \tag{6}$$

In the formula, $P_{j,i}$ denotes the total number of people on the bus route numbered j in the i time period and n is the sum of the bus routes. The principal components are calculated as follows: the original variables are standardised, the correlation matrix between the variables is calculated, the eigenroots and eigenvectors of this matrix are calculated, and the principal components are determined by size ranking. The number of principal components is determined by the cumulative contribution rate. Generally, if the cumulative rate reaches or exceeds 70%, then the top n components are retained. The variance contribution of the principal components is shown in Eq (7):

$$\lambda_i / \sum_{i=1}^{p} x_i \tag{7}$$

where λ_i represents the ratio of the variance of the principal component Z_i to the total variance. A larger ratio indicates that Z_i is better able to synthesise the original information.

Step 3: Passenger flow forecast

Step 3.1: The short time series clustering Seasonal Autoregressive Integrated Moving Average passenger flow forecasting model is built based on the results from Steps 1 and 2. Figure 1 shows the modeling process.

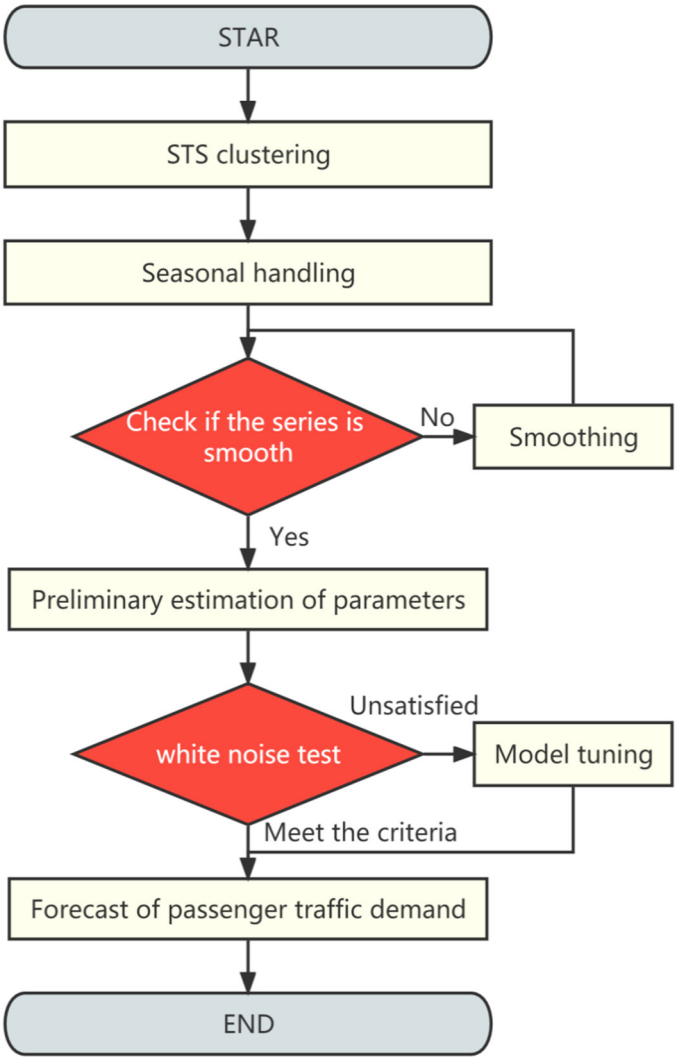

Figure 1. General steps of STSC-SARIMA model passenger flow forecasting.

The STSC-SARIMA modelling first uses STS clustering to process the irregular components of the time series. Seasonal adjustments are then applied to remove seasonal effects to obtain a standard dataset. Second, the data set is tested for smoothness. If the series does not satisfy the smoothing condition, the series is made to satisfy the smoothing condition using a d-order difference or other

methods. The p and q values of the ARIMA model are determined using statistics that describe the characteristics of the series, such as correlation coefficients (autocorrelation, deviation correlation). The process follows the principle of having few parameters. Finally, the unknown parameters of the model are estimated and tested for significance and reasonableness using p and q values.

Step 3.2: Validation of the accuracy of the model fit. The validation method introduces both Mean Absolute Error (MAE) and Root Mean Square Error (RMSE), expressed in Eqs (8) and (9), respectively. Larger values of these error measures are associated with a greater prediction error; smaller values indicate a higher accuracy [54]. In this paper, the mean absolute percentage error (MAPE), expressed in Eq (10), is used as the measurement standard. In general, a prediction accuracy of 80% or more meets the needs of passenger flow prediction; a prediction accuracy of over 90% indicates a highly accurate prediction [55].

$$MAE = \frac{1}{N}\sum_{i=1}^{n}\left|y_p(d) - y_r(d)\right| \tag{8}$$

$$RMSE = \sqrt{\frac{1}{N}\sum_{i=1}^{n}\left(y_p(d) - y_r(d)\right)^2} \tag{9}$$

$$MAPE = \frac{1}{N}\sum_{i=1}^{n}\left|\frac{y_p(d)-y_r(d)}{y_r(d)}\right| \tag{10}$$

where $y_p(d)$ denotes the predicted value of the elderly passenger flow obtained from the model fit, respectively, and N is the total number of days. $y_r(d)$ is the real data obtained by bringing the parameters obtained by clustering into the bus trip data of the elderly.

4. Experimental simulation

4.1. Data sources

This study analysed data on public transport trips taken by older people in Lhasa from October 2018 to February 2020. Lhasa is a typical plateau city in Tibet with a long history and cultural heritage. It is subject to geographical constraints and cultural influences, and the situation created by having an aging population is becoming increasingly serious [56−58]. There are currently 73,700 elderly people over 60 years of age in Lhasa, accounting for approximately 24% of the city's population. The topography and traffic pressures are exacerbated by the intensifying conflict between the supply and demand of public transport services, due to the city's increasing aging. The predominance of conventional public transport for older people in Lhasa, with 38 bus routes operating in the city centre, provides data to support this choice of study population.

4.2. Spatiotemporal features

4.2.1. Seasonal characteristics

An integer multiple of 5 minutes (parameter) was selected as the test time period. After setting the parameter, 7 days of data were randomly selected for data processing to determine the average slope for each day of the corresponding time period. Finally, the time period parameter and output

were determined in 15-minute intervals. The statistical time range for each day was set to 6:30 am−22:30pm, and the output was averaged by month. The results show that between 6:30−7:30 am, the number of older people travelling was above the annual average in May-September and remained in a stable range for January-April and October-December. In contrast, the last hour of the day had a more stable number of people from January to April and October to December, with a cut-off time period of 21:30−21:45 pm. The cut-off time for older people travelling on the bus from May to September was delayed by half an hour, from 22:00−22:15 pm. In these months, the numbers levelled off and were generally higher than in other months. This is consistent with the pattern that older people's bus travel is influenced by seasonal characteristics [59].

4.2.2. Temporal characteristics

In this paper, data from October 2018 to January 2020 were selected for the HP filtering analysis. Figure 2 shows the HP filtering results, where the Roman value represents three consecutive months (individually expressed in January 2020); and S represents the original series. The trendline is shown in the top half of the figure and the periodicity is shown in the bottom half of the figure.

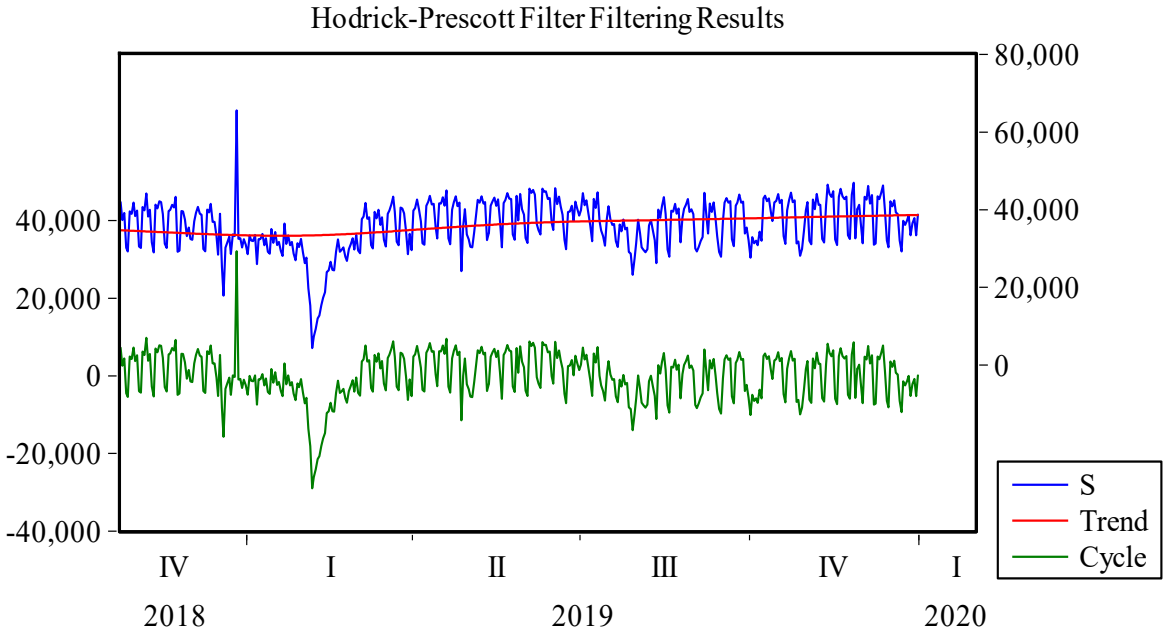

Figure 2. H-P filter analysis diagram.

Figure 3 shows the overall upward trend and cyclical change in the number of older people travelling by public bus. This reflects the increasing aging of Lhasa and the overall increasing demand for public transport. To further determine the specific parameters of the cyclical variation characteristics, we performed BP filtering on the January to December 2019 data. The filtering method was the fixed length symmetric method (Baxter-King). Figure 3 shows the results. Figure 3(a) represents the original sequence, the acyclic sequence, and the cyclic sequence from top to bottom. Figure 3(b) provides the frequency response function with the interval of frequencies that depicts the results for the ideal case and the realistic case. The original sequence, the acyclic sequence, and the

cyclic sequence are represented from top to bottom in Figure 3(a), and the frequency response function $\Omega(\omega)$ is given in Figure 3(b). The interval of the frequency ω is $[0, 0.5]$, depicting the results for both ideal and realistic situations. The results show that the greatest weight is associated with days 6 to 8. This indicates that the flow of elderly travelers in Lhasa fluctuates cyclically over a range of 6 to 8 days. This largely coincides with the change in the 7-day cycle of travel for older people [60].

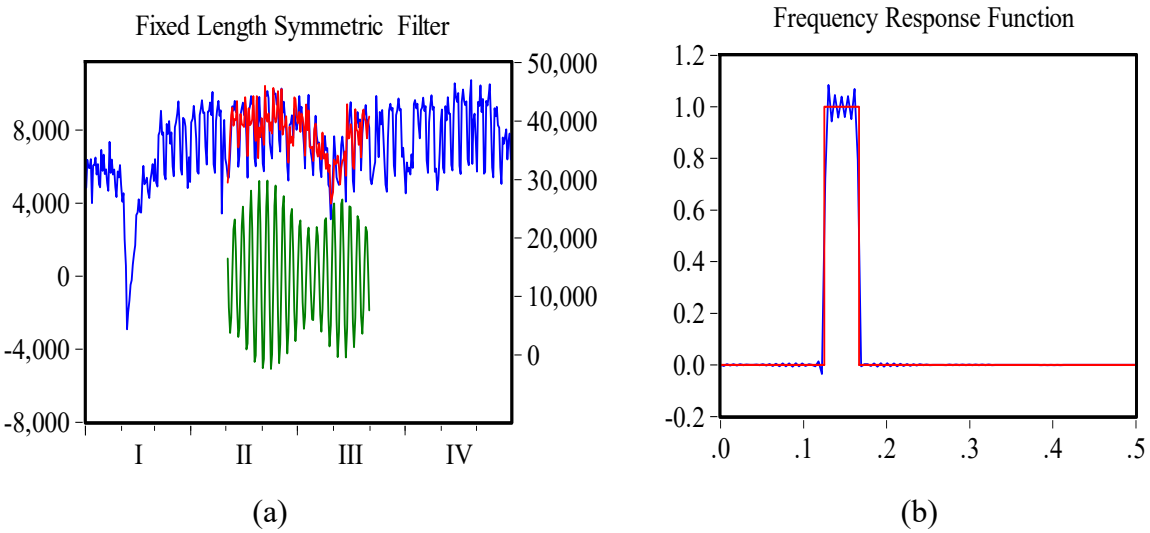

Figure 3. BP filter decomposition diagram.

This study also evaluated the temporal variation in the characteristics of daily bus travel among older adults. The data were averaged over three randomly selected days in the first, middle, and third part of each month. The monthly fluctuations were also found to be consistent, with the number of older people travelling at each time of day varying consistently from January to April, May to September, and October to December. Figure 4(a) shows the average data for these groupings (January-April, May-September, and October-December), while Figure 4(b) shows the data for 8 randomly selected days from the full year of data. There were three daily peak times for public transport for older people in Lhasa: 7:00−7:30 am for the first peak, 9:00−11:30 am for the second peak, and 16:30−18:00 pm for the third peak. The first peak phase (7:00−7:30 am) had the fastest growth in the number of trips; the second peak phase (9:00−11:30 am) had the maximum number of trips for the day; and the third peak phase (16:30−18:00 pm) was a small wave. These results were generally consistent those of Wang et al. [61]. The overall shift in the travel time curve for seniors from May to September, compared to other months, may have been due to the gradual warming of temperatures in the northern hemisphere during this period.

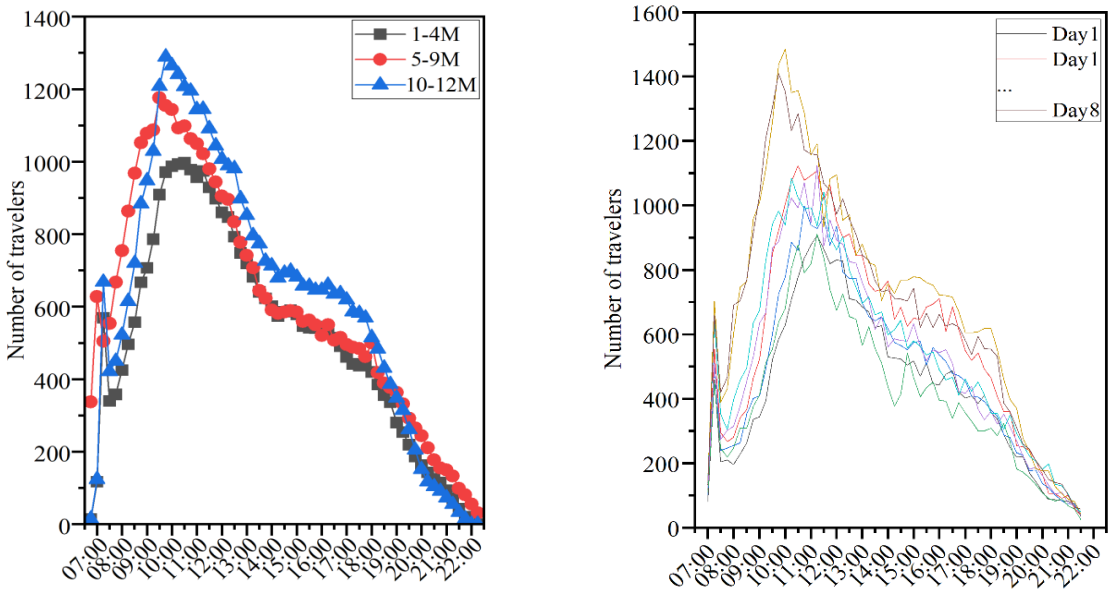

Figure 4. Daily bus trip data for the elderly.

4.2.3. Bus route load factor

The data for all bus routes were collated for nine days randomly selected from the monthly data for 2019. The average of the number of older people on all bus routes was first calculated for 108 days over 12 months; then, the proportion of passengers carried on each route was identified. The results show that the average daily number of senior citizen trips was significantly higher for bus lines 16 and 20 compared to other bus routes, accounting for 8.8 and 9.6% of the total senior trips, respectively. The load factor of all bus lines was roughly divided into three levels: a lower level with a load factor of 0 to 1.2%; a moderate level with a load factor of 1.2 to 2.4%; and a high level with a load factor of 2.4 to 9.6%.

Routes with high levels of load factor were randomly selected for principal component analysis. KMO and Bartlett's test calculated the KMO statistic as 0.77, which was greater than the minimum standard of 0.5. The Bartlett's spherical test showed that the original hypothesis of the correlation matrix did not hold, $p < 0.001$. This indicated that it could be analysed using principal component analysis. In this analysis, the first three principal components had eigenvalues greater than 1 and a cumulative contribution of 91.169%. As such, the first three common factors were selected. The results of the common factor variance ratios found that the common method for each indicator variable was above 0.5 and most were close to 0.9. This indicated that the three common factors effectively reflected most of the information in the original data. Table 2 shows the rotated factor loadings, where the bus route numbers are denoted by Xn. After rotation, each route had a larger loading on factor 1. Comparing this result with the load rate of each line revealed that the order of the load of the above line on factor 1 was consistent with the order of the passenger flow load.

Table 2. Factor loadings after rotation.

	Original		Rescale	
	Ingredient 1	Ingredient 2	Ingredient 1	Ingredient 2
X24	275.829	-18.265	0.96	-0.064
X18	260.362	8-48.046	0.95	-0.175
X2	247.675	38.784	0.921	0.144
X14	167.673	19.876	0.89	0.106
X7	271.644	-102.998	0.882	-0.334
X28	204.699	-23.821	0.828	-0.096
X17	42.904	305.072	0.133	0.946
X23	-60.055	224.74	-0.219	0.819

To analyse whether the size of the passenger flow was related to the population centres and the main commercial centres and to verify travel demand, Figure 5 was generated using geographical elements and data for bus routes 1, 2, 16, 20, and 24, and the bus routes with high passenger load factors.

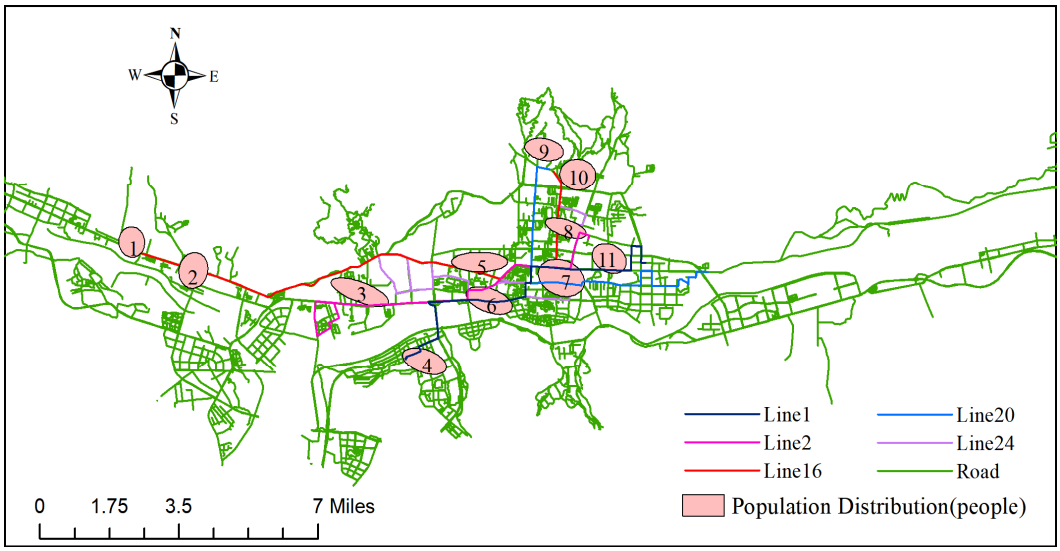

Figure 5. Map of population distribution and bus routes.

Figure 5 shows that the dense roads are mostly commercial areas. The main residential areas are marked with 11 numbers. Areas 1, 3, 4, and 6 each have populations between 2000 and 5754 people. Area 8 has a population of around 70,000; the remaining areas each have populations of between 10,000 and 30,000 people. Figure 5 shows that, for the elderly, the routes with high passenger load factors mostly run through most commercial areas and populated areas. Most studies have found that older people's activities are mainly located in large shopping malls, shopping centres, scenic areas, and near primary schools, where they shop, entertain themselves, and take children to and from school [62].

4.3. Prediction model development and results

This section focuses on a case study of three randomly selected bus routes with high load factors: routes 16, 20, and 24. The daily bus loads for the elderly were modeled at different times of the day (at 15 minute intervals) for May, June, and July 2019. The ratio of the test set to the validation set was set at 4:1. The data from May and June were used as the training set to predict the three peak hours of traffic for the first 14 days (two weeks) of July. First, four data sets from bus route 16 were selected for the comparative analysis of the model fit. Data sets 1 and 2 were for 8:30−9:00 am and 9:00−9:45 am. The other two data sets (data sets 3 and 4) were for 10:45−11:15 am and 14:15−14:45 pm. The difference between the data sets was that the sizes of the slope values in the clustering module were similar for data sets 1, 2, and 4 when using 15 minute intervals; however, the slope values for data set 3 differed. In the model optimisation stage, this experiment first identified three models. Then, the optimal model was determined by adjusting R2, AIC, SC, and the correlation of the residual series for comparison. Table 3 shows the fitting results for the data sets.

Table 3. Estimated ARIMA models.

Model	AIC	SC	F-statistic	R-squared
ARIMA (4, 2, 2)	15.043	15.290	3.102 (0.254)	6.458 (0.239)
ARIMA (1, 0, 1)	19.027	19.131	0.643 (0.530)	1.368 (0.504)
ARIMA (1, 0, 2)	10.132	10.271	0.276 (0.759)	0.606 (0.739)
ARIMA (2, 0, 1)	9.576	9.715	0.344 (0.710)	0.631 (0.729)

Note: AIC and SC represent Akaike Info Criterion and Schwarz Criterion; respectively; the F-statistic and R-squared values were generated using the Breusch-Godfrey serial correlation linear model (LM) test (where the LM statistics all exceed 10%, indicating that the model residual series are not correlated).

Once the model was built, the fitting order followed the model building order, starting with one data set and going to the fourth data set to obtain Figure 6(a)−(d). The results show that the MAE and RMSE values of the two model fits were closer when the slopes of the 15 minute time periods of the first and second data sets were similar, and when the fluctuation intervals of the passenger flow sizes were essentially the same. When the range of fluctuation in passenger flow across the third and fourth data sets was basically the same, the third data set had a larger slope difference compared with the fourth data set, when 15 minutes was used as the interval. The MAE was higher by 0.143 and RMSE was higher by 0.077. Therefore, splitting the time series at 15 minute intervals, when the slope values were close to each other, yielded better predictions.

In fitting the model to elderly passenger flows on bus routes 16, 20, and 24, the time periods were chosen to minimize the fluctuation of the slope (15 minute intervals) based on the experimental results. The final three peak hours identified as good fits were 6:30−7:30 am, 8:30−11:30 am, and 16:30−18:00 pm. These were determined using a combination of data from the three routes. Table 4 shows the modelling results, again using May and June as the training set and the first two weeks of July as the validation set for the fitted data.

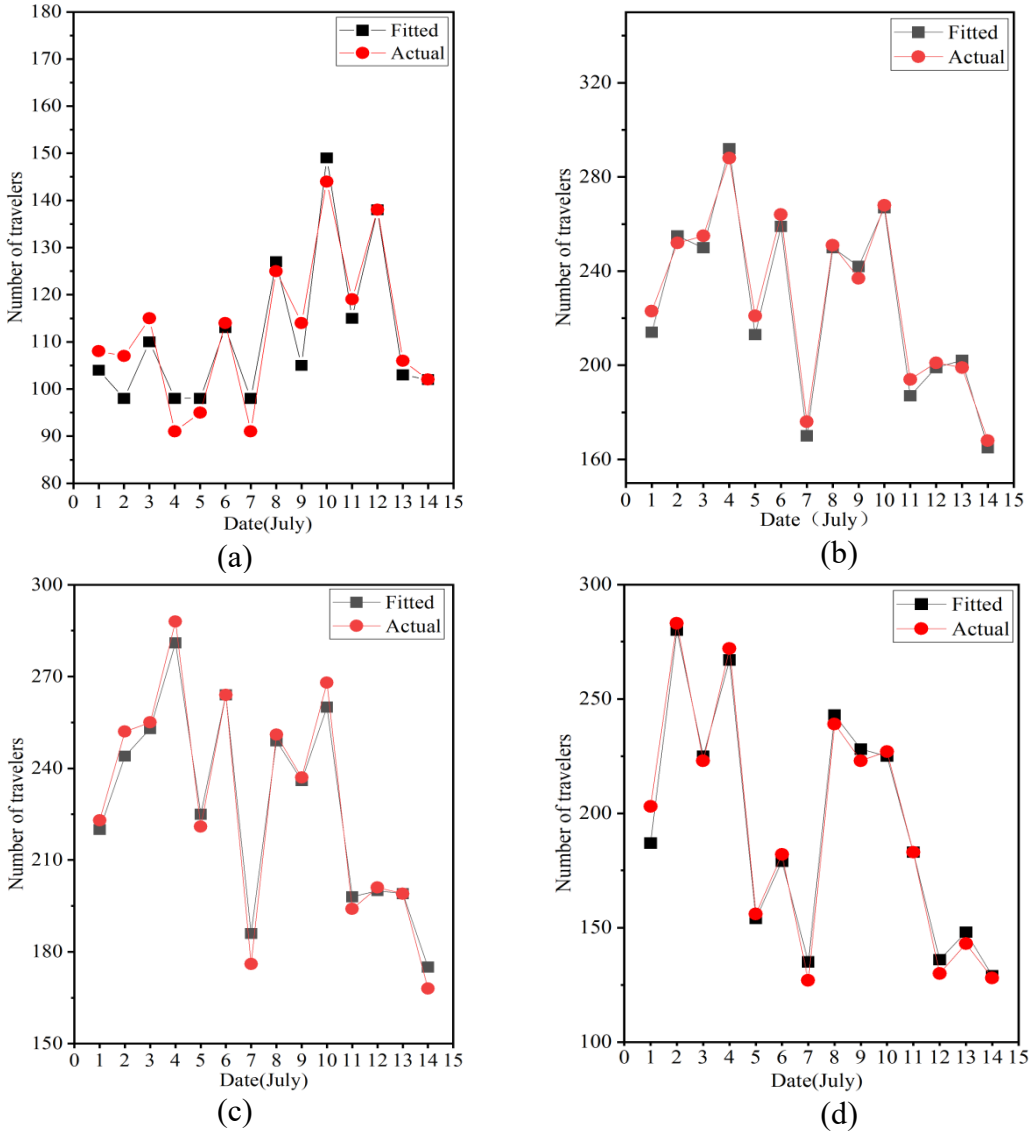

Figure 6. Fitted data and real data for four periods of road vehicles.

Table 4. Peak period modeling for three bus lines.

Line	Period	Model	AIC	SC	SC	R-squared
	6:30−7:30	ARIMA (2, 0, 0)	11.112	11.253	1.395 (0.257)	2.867 (0.239)
16	8:00−11:30	ARIMA (2, 2, 1)	12.809	12.913	0.692 (0.505)	1.462 (0.481)
	16:30−18:00	ARIMA (1, 0, 2)	11.214	11.352	0.039 (0.969)	0.084 (0.959)
	6:30−7:30	ARIMA (1, 1, 1)	9.538	9.642	0.794 (0.457)	1.683 (0.431)
20	8:00−11:30	ARIMA (3, 0, 1)	13.165	13.338	0.916 (0.406)	1.976 (0.372)
	16:30−18:00	ARIMA (4, 2, 2)	15.043	15.290	3.102 (0.254)	6.458 (0.239)
	6:30−7:30	ARIMA (1, 0, 1)	19.027	19.131	0.643 (0.530)	1.368 (0.504)
24	8:00−11:30	ARIMA (1, 0, 2)	10.132	10.271	0.276 (0.759)	0.606 (0.739)
	16:30−18:00	ARIMA (2, 0, 1)	9.576	9.715	0.344 (0.710)	0.631 (0.729)

The corresponding data were imported through the established model, and the MAE, RSME, and

MAPE were calculated as shown in Table 5.

Table 5. Peak fitting results of three bus lines.

Line	Period	Model	MAE	RMSE	MAPE
	6:30−7:30	ARIMA (2, 0, 0)	4.286	5.014	0.033
16	8:00−11:30	ARIMA (2, 2, 1)	7.643	8.379	0.006
	16:30−18:00	ARIMA (1, 0, 2)	4.214	4.862	0.017
	6:30−7:30	ARIMA (1, 1, 1)	4.357	5.339	0.041
20	8:00−11:30	ARIMA (3, 0, 1)	7.429	8.168	0.005
	16:30−18:00	ARIMA (4, 2, 2)	4.387	5.119	0.015
	6:30−7:30	ARIMA (1, 0, 1)	4.013	4.942	0.039
24	8:00−11:30	ARIMA (1, 0, 2)	6.785	7.903	0.006
	16:30−18:00	ARIMA (2, 0, 1)	4.115	4.879	0.018

Numerical experimental results show that the prediction model used in this study exceeds a 90% prediction accuracy. The average MAE and RMSE of the predicted and actual values remain between 5.25 and 6.07, demonstrating the applicability and reliability of the method.

In addition, in order to verify the predictive performance of this model, a convolutional neural network was designed for this situation. The training set and test set were the same, with the addition of initial data normalization and de-normalization of prediction results. The deep convolutional neural network had a 6-layer structure, including a convolutional layer, pooling layer, fully connected layer, Flatten layer, and Dropout layer. The learning rate was set to 0.2, and the prediction effect was better when 0.05 was selected for the Dropout layer after many tests. The optimizer adopted the stochastic gradient descent (SGD) method, and the number of iterations was selected 300 times.

The data results show that STSC-SARIMA reduces the average MAE by 0.23% and the average RMSE by 0.91% compared to the convolutional neural network model predictions.

5. Conclusions

Accurately analyzing the passenger flow characteristics of the elderly forms the basis for generating valid travel demand forecasts. Together, they provide a solid theoretical basis to develop new public transport travel strategies for older people. Based on the four principal components of the time series (trend, cycle, season, and an irregular component), this paper analyzed the spatiotemporal characteristics of elderly people who take buses, and proposed a passenger flow prediction method using the STSC-SARIMA model. The elderly passenger demand forecasting method proposed in this paper enables the efficient and accurate forecasting of elderly passenger demand, using seasonal moving autoregressive models incorporating clustering techniques and smart bus card data. The method has the following advantages.

1) Using original data from bus smart cards of the elderly eliminates the problematic influence of personal data, enabling the construction of a unified and effective data set to analyse, predict, and validate passenger flow. The historical data span one year, and are stored by months, days, and minutes to support retrieval and analysis.

2) This paper analyzed the temporal and spatial characteristics of buses and passenger flow. There are significant differences in the passenger flow of the elderly in different population areas and on

different bus lines. The bus routes with high load factors clearly run through major population and commercial centres. Analysing the spatial and temporal characteristics of passenger flows clearly reflects the travel needs of older people and is the focus of passenger flow forecasting.

3) The short-time clustering method effectively addresses the irregular components contained in the time series. Combining this with the seasonal differential moving autoregressive model enables the method to effectively address the trend, cycle, and seasonal components of the time series.

4) Compared to most experiments, where only cross-sectional data are fitted, the choice to include a spatio-temporal analysis of passenger flows to validate demand and forecast passenger flows is more practical and applicable for addressing travel pressures and providing travel security for older people.

The research described in this paper highlights options for policymakers or operators wishing to facilitate the travel of groups of the elderly. This could also reduce operating costs or save operator funds. For example, the passenger load ratio of a bus route can be used to analyze time and space factors to determine elderly travel demands. This could inform the design of dedicated bus lines for the elderly or lead to more effective schedules.

There remain opportunities for future research using the methods described in this study. For example, studies with too large a scope or too much data may require more time to generate predictions. As such, data processing should be further optimised. Combining the latest neural network model and forming a feature multi-label input on the basis of this experiment is a possible research direction to improve prediction performance.

Acknowledgments

This research was supported by the National Natural Science Foundation of China (Grant No. 51968063), Academic development support program for young doctors of Tibet University (No. zdbs202212 and No. zdbs202229), Himalayan human activities and regional development collaborative innovation construction center project (No. 00060872), Tibet University Plateau Train Operation Control Simulation Platform Scientific Research Innovation Team Construction Project and the Fundamental Maintenance Project of Plateau Major Infrastructure and Environment Real-time Online Monitoring Center.

Conflict of interest

The authors declare there is no conflict of interest.

References

1. Y. Zhang, E. Yao, R. Zhang, H. Xu, Analysis of elderly people's travel behaviours during the morning peak hours in the context of the free bus programme in Beijing, China, *J. Transp. Geogr.*, **76** (2019), 191–199. https://doi.org/10.1016/j.jtrangeo.2019.04.002
2. P. Thaithatkul, S. Chalermpong, W. Laosinwattana, H. Kato, Mobility, activities, and happiness in old age: case of the elderly in Bangkok, *Case Stud. Transp. Policy*, **10** (2022), 1462–1471. https://doi.org/10.1016/j.cstp.2022.05.010

3. A. Jones, A. Goodman, H. Roberts, R. Steinbach, J. Green, Entitlement to concessionary public transport and wellbeing: a qualitative study of young people and older citizens in London, UK, *Social Sci. Med.*, **91** (2013), 202–209. https://doi.org/10.1016/j.socscimed.2012.11.040
4. F. Shao, Y. Sui, X. Yu, R. Sun, Spatio-temporal travel patterns of elderly people–A comparative study based on buses usage in Qingdao, China, *J. Transp. Geogr.*, **76** (2019), 178–190. https://doi.org/10.1016/j.jtrangeo.2019.04.001
5. J. R. Hjorthol, L. Levin, A. Sirén, Mobility in different generations of older persons: the development of daily travel in different cohorts in Denmark, Norway and Sweden, *J. Transp. Geogr.*, **18** (2010), 624–633. https://doi.org/10.1016/j.jtrangeo.2010.03.011
6. J. Kim, D. J. Schmöcker, T. Nakamura, N. Uno, T. Iwamoto, Integrated impacts of public transport travel and travel satisfaction on quality of life of older people, *Transp. Res. Part A: Policy Pract.*, **138** (2020), 15–27. https://doi.org/10.1016/j.tra.2020.04.019
7. X. Dong, Addressing health and well-being of U.S. Chinese older adults through community-based participatory research: introduction to the PINE study, *AIMS Med. Sci.*, **2** (2015), 261–270. https://doi.org/10.3934/medsci.2015.3.261
8. C. Dillon, F. E. Taragano, Activity and lifestyle factors in the elderly: their relationship with degenerative diseases and depression, *AIMS Med. Sci.*, **3** (2016), 213–216. https://doi.org/10.3934/medsci.2016.2.213
9. S. Zhang, P. Jing, D. Yuan, C. Yang, On parents' choice of the school travel mode during the COVID-19 pandemic, *Math. Biosci. Eng.*, **19** (2022), 9412−9436. https://doi.org/10.3934/mbe.2022438
10. X. Hu, J. Wang, L. Wang, Understanding the travel behavior of elderly people in the developing country: a case study of Changchun, China, *Procedia - Social Behav. Sci.*, **96** (2013), 873–880. https://doi.org/10.1016/j.sbspro.2013.08.099
11. J. Mak, L. Carlile, S. Dai, Impact of population aging on Japanese international travel to 2025, *J. Travel Res.*, **44** (2005), 151–162. https://doi.org/10.1177/0047287505278993
12. M. Wei, T. Liu, B. Sun, Optimal routing design of feeder transit with stop selection using aggregated cell phone data and open source GIS tool, *IEEE Trans. Intell. Transp. Syst.*, **22** (2021), 2452–2463. https://doi.org/10.1109/TITS.2020.3042014
13. M. Wei, B. Jing, J. Yin, Y. Zang, A green demand-responsive airport shuttle service problem with time-varying speeds, *J. Adv. Transp.*, **2020** (2020), 1–13. https://doi.org/10.1155/2020/9853164
14. M. Wei, T. Liu, B. Sun, B. Jing, Optimal integrated model for feeder transit route design and frequency-setting problem with stop selection, *J. Adv. Transp.*, **2020** (2020), 1–12. https://doi.org/10.1155/2020/6517248
15. Y. Hou, Polycentric urban form and non-work travel in Singapore: a focus on seniors, *Transp. Res. D Transp. Environ.*, **73** (2019), 245–275. https://doi.org/10.1016/j.trd.2019.07.003
16. J. Tang, J. Liang, F. Liu, J. Hao, Y. Wang, Multi-community passenger demand prediction at region level based on spatio-temporal graph convolutional network, *Transp. Res. Part C: Emerging Technol.*, **124** (2019), 1–18. https://doi.org/10.1016/j.trc.2020.102951
17. S. Halyal, R. H. Mulangi, M. M.Harsha, Forecasting public transit passenger demand: With neural networks using APC data, *Case Stud. Transp. Policy*, **10** (2022), 965–975. https://doi.org/10.1016/j.cstp.2022.03.011

18. Y. Feng, J. Hao, X. Sun, J. Li, Forecasting short-term tourism demand with a decomposition-ensemble strategy, *Procedia Comput. Sci*., **199** (2022), 879–884. https://doi.org/10.1016/j.procs.2022.01.110
19. Y. Bai, Z. Sun, B. Zeng, J. Deng, C. Li, A multi-pattern deep fusion model for short-term bus passenger flow forecasting, *Appl. Soft Comput*., **58** (2017), 669–680. https://doi.org/10.1016/j.asoc.2017.05.011
20. G. Lin, A. Lin, D. Gu, Using support vector regression and K-nearest neighbors for short-term traffic flow prediction based on maximal information coefficient, *Inf. Sci*., **608** (2022), 517–531. https://doi.org/10.1016/j.ins.2022.06.090
21. O. Giraka, K. V. Selvaraj, Short-term prediction of intersection turning volume using seasonal ARIMA model, *Transp. Lett*., **2019** (2019), 483–490. https://doi.org/10.1080/19427867.2019.1645476
22. A. Emami, M. Sarvi, S. A. Bagloee, Short-term traffic flow prediction based on faded memory Kalman Filter fusing data from connected vehicles and Bluetooth sensors, *Simul. Modell. Pract. Theory*, **102** (2020), 1–17. https://doi.org/10.1016/j.simpat.2019.102025
23. V. S. Kumar, Traffic flow prediction using Kalman filtering technique, *Procedia Eng*., **187** (2017), 582–587. https://doi.org/10.1016/j.proeng.2017.04.417
24. Z. Shi, N. Zhang, P. M. Schonfeld, J. Zhang, Short-term metro passenger flow forecasting using ensemble-chaos support vector regression, *Transp. A: Transp. Sci.*, **16** (2019), 194–212. https://doi.org/10.1080/23249935.2019.1692956
25. Y. Sun, B. Leng, W. Guan, A novel wavelet-SVM short-time passenger flow prediction in Beijing subway system, *Neurocomputing*, **166** (2015), 109–121. https://doi.org/10.1016/j.neucom.2015.03.085
26. Y. Liu, Z. Liu, R. Jia, DeepPF: a deep learning based architecture for metro passenger flow prediction, *Transp. Res. Part C: Emerging Technol.*, **101** (2019), 18–34, https://doi.org/10.1016/j.trc.2019.01.027
27. C. W. Tsai, C. H. Hsia, S. J. Yang, S. J. Liu, Z. Y. Fang, Optimizing hyperparameters of deep learning in predicting bus passengers based on simulated annealing, *Appl. Soft Comput.*, **88** (2020), 18–34. https://doi.org/10.1016/j.asoc.2020.106068
28. B. Sun, T. Sun, P. Jiao, Spatio-temporal segmented traffic flow prediction with ANPRS data based on improved XGBoost, *J. Adv. Transp.*, **2021** (2021), 1–24. https://doi.org/10.1155/2021/5559562
29. J. J. Buckley, Y. Hayashi, Fuzzy neural networks: a survey, *Fuzzy Sets Syst*., **66** (1994), 1–13. https://doi.org/10.1016/0165-0114(94)90297-6
30. H. Peng, H. Wang, B. Du, M. Z. A. Bhuiyan, H. Ma, J. Liu, et al., Spatial temporal incidence dynamic graph neural networks for traffic flow forecasting, *Inf. Sci*., **521** (2020), 277–290. https://doi.org/10.1016/j.ins.2020.01.043
31. X. Yang, Q. Xue, X. Yang, H. Yin, Y. Qua, X. Li, et al., A novel prediction model for the inbound passenger flow of urban rail transit, *Inf. Sci*., **566** (2021), 347–363. https://doi.org/10.1016/j.ins.2021.02.036
32. X. Fu, Y. Zuo, J. Wu, Y. Yuan, S. Wang, Short-term prediction of metro passenger flow with multi-source data: a neural network model fusing spatial and temporal features, *Tunnelling Underground Space Technol.*, **124** (2022), 1–15. https://doi.org/10.1016/j.tust.2022.104486

33. L. Liu, C. R. Chen, A novel passenger flow prediction model using deep learning methods, *Transp. Res. Part C: Emerging Technol.*, **84** (2017), 74–91. https://doi.org/10.1016/j.trc.2017.08.001
34. D. Luo, D. Zhao, Q. Ke, X. You, L. Liu, H. Ma, Spatiotemporal hashing multigraph convolutional network for service-level passenger flow forecasting in bus transit systems, *IEEE Internet Things J.*, **9** (2021), 6803–6815. https://doi.org/10.1109/JIOT.2021.3116241
35. Y. Gao, Z. Guo, Y. Long, Z. Cui, X. Li, Passengers' travel behavior before and after the adjustment of regular bus collinear sections: a case study in the incipient phase of metro operation in Xiamen, *Travel Behav. Soc.*, **26** (2022), 221–230. https://doi.org/10.1016/j.tbs.2021.10.006
36. Y. Yang, M. Cao, L. Cheng, K. Zhai, X. Zhao, J. D. Vos, Exploring the relationship between the COVID-19 pandemic and changes in travel behaviour: a qualitative study, *Transp. Res. Interdiscip. Perspect.*, **11** (2021), 1–4. https://doi.org/10.1016/j.trip.2021.100450
37. S. Hu, Q. Liang, H. Qian, J. Weng, W. Zhou, Frequent-pattern growth algorithm based association rule mining method of public transport travel stability, *Int. J. Sustainable Transp.*, **15** (2021), 879–892. https://doi.org/10.1080/15568318.2020.1827318
38. Z. Ma, J. Xing, M. Mesbah, L. Ferreira, Predicting short-term bus passenger demand using a pattern hybrid approach, *Transp. Res. Part C: Emerging Technol.*, **39** (2014), 148–163. https://doi.org/10.1016/j.trc.2013.12.008
39. N. Oort, T. Brands, E. Romph, Short-term prediction of ridership on public transport with smart card data, *Transp. Res. Rec.*, **2535** (2015), 105–111. https://doi.org/10.3141/2535-12
40. I. Okutani, Y. J. Stephanedes, Dynamic prediction of traffic volume through Kalman filtering theory, *Transp. Res. Part B: Methodol.*, **18** (1984), 1–11. https://doi.org/10.1016/0191-2615(84)90002-X
41. W. Min, L. Wynter, Real-time road traffic prediction with spatio-temporal correlations, *Transp. Res. Part C: Emerging Technol.*, **19** (2011), 606–616. https://doi.org/10.1016/j.trc.2010.10.002
42. Y. K. Chan, S. T. Dillon, J. Singh, E. Chang, Neural-network-based models for short-term traffic flow forecasting using a hybrid exponential smoothing and Levenberg–Marquardt algorithm, *IEEE Trans. Intell. Transp. Syst.*, **13** (2012), 644–654. https://doi.org/10.1109/TITS.2011.2174051
43. R. Xue, J. D. Sun, S. Chen, Short-term bus passenger demand prediction based on time series model and interactive multiple model approach, *Discrete Dyn. Nat. Soc.*, **2015** (2015), 1–11. https://doi.org/10.1155/2015/682390
44. F. Toqué, M. Khouadjia, E. Come, M. Trepanier, L. Oukhellou, Short & long term forecasting of multimodal transport passenger flows with machine learning methods, in *2017 IEEE 20th International Conference on Intelligent Transportation Systems (ITSC)*, **2017** (2017), 560–566. https://doi.org/10.1109/ITSC.2017.8317939
45. C. Li, X. Wang, Z. Cheng, Y. Bai, Forecasting bus passenger flows by using a clustering-based support vector regression approach, *IEEE Access*, **8** (2020), 19717–19725. https://doi.org/10.1109/ACCESS.2020.2967867
46. F. Jiao, L. Huang, Z. Gao, Multi-step time series forecasting of bus passenger flow with deep learning methods, in *Liss 2020*, **2021** (2021), 539–553. https://doi.org/10.1007/978-981-33-4359-7_38

47. W. Lv, Y. Lv, Q. Ouyang, Y. Ren, A bus passenger flow prediction model fused with point-of-interest data based on extreme gradient boosting, *Appl. Sci.*, **12** (2022), 1–14. https://doi.org/10.3390/app12030940
48. Z. Gan, T. Feng, Y. Wu, M. Yang, H. Timmermans, Station-based average travel distance and its relationship with urban form and land use: an analysis of smart card data in Nanjing City, China, *Transp. Policy*, **79** (2019), 137–154. https://doi.org/10.1016/j.tranpol.2019.05.003
49. J. Yong, L. Zheng, X. Mao, X. Tang, A. Gao, W. Liu, Mining metro commuting mobility patterns using massive smart card data, *Physica A*, **584** (2021), 1–16. https://doi.org/10.1016/j.physa.2021.126351
50. O. Egu, P. Bonnel, Investigating day-to-day variability of transit usage on a multimonth scale with smart card data. A case study in Lyon, *Travel Behav. Soc.*, **19** (2020), 112–123. https://doi.org/10.1016/j.tbs.2019.12.003
51. E. F. Grubbs, Sample criteria for testing outlying observations, *Ann. Math. Stat.*, **21** (1950), 27–58. https://www.jstor.org/stable/2236553
52. C. S. Möller-Levet, F. Klawonn, H. K. Cho, O. Wolkenhauer, Fuzzy clustering of short time-series and unevenly distributed sampling points, *Adv. Intell. Data Anal.*, **2810** (2003), 330–340 https://doi.org/10.1007/978-3-540-45231-7_31
53. J. R. Hodrick, C. E. Prescott, Postwar US business cycles: an empirical investigation, *J. Money Credit Banking*, **29** (1997), 1–16. https://doi.org/10.2307/2953682
54. H. Zhai, L. Cui, Y. Nie, X. Xu, W. Zhang, A comprehensive comparative analysis of the basic theory of the short term bus passenger flow prediction, *Symmetry*, **10** (2018), 1–23. https://doi.org/10.3390/sym10090369
55. L. hang, Q. Liu, W. Yang, N. Wei, D. Dong, An improved k-nearest neighbor model for short-term traffic flow prediction, *Procedia - Social Behav. Sci.*, **96** (2013), 653–662. https://doi.org/10.1016/j.sbspro.2013.08.076
56. G. Cheng, S. Zhao, J. Li, The effects of latent attitudinal variables and sociodemographic differences on travel behavior in two small, underdeveloped cities in China, *Sustainability*, **11** (2019), 1–17. https://doi.org/10.3390/su11051306
57. G. Cheng, S. Jiang, T. Zhang, Fuzzy multidimensional assessment approach of travel deprivation in small underdeveloped cities: case study of Lhasa, China, *J. Adv. Transp*., **2021** (2021), 1–12. https://doi.org/10.1155/2021/8851449
58. G. Cheng, L. Guo, T. Zhang, Spatial equity assessment of bus travel behavior for pilgrimage: evidence from Lhasa, Tibet, China, *Sustainability*, **14** (2022), 1–15. https://doi.org/10.3390/su141710486
59. S. Liu, T. Yamamoto, E. Yao, T. Nakamura, Examining public transport usage by older adults with smart card data: a longitudinal study in Japan, *J. Transp. Geogr*., **93** (2021), 1–12. https://doi.org/10.1016/j.jtrangeo.2021.103046
60. A. Barnett, E. Cerin, C. M. Cheung, H. C. Sit, J. D. Macfarlane, M. W. Chan, Reliability and validity of the IPAQ-L in a sample of Hong Kong urban older adults: does neighborhood of residence matter, *J Aging Phys. Act.*, **20** (2012), 402–420. https://doi.org/10.1123/japa.20.4.402
61. H. Wang, L. Fu, Y. Zhou, H. Li, Modelling of the fuel consumption for passenger cars regarding driving characteristics, *Transp. Res. Part D: Transp. Environ*., **13** (2008), 479–482. https://doi.org/10.1016/j.trd.2008.09.002

62. R. Mackett, Improving accessibility for older people–Investing in a valuable asset, *J. Transp. Health*, **2** (2015), 5–13. https://doi.org/10.1016/j.jth.2014.10.004

AIMS Press